

Uniquely folded shapes, photophysical properties, and recognition abilities of macrocyclic BODIPY oligomers

著者 (英)	Tomohiro Hojo, Takashi NAKAMURA, Ryota MATSUOKA, Tatsuya NABESHIMA
journal or publication title	Heteroatom chemistry
volume	29
number	5-6
page range	e21470
year	2018-12
権利	(C) 2018 Wiley Periodicals, Inc. This is the peer reviewed version of the following article: Heteroatom Chemistry Volume29 Issue5-6 e21470, which has been published in final form at https://doi.org/10.1002/hc.21470 . This article may be used for non-commercial purposes in accordance with Wiley Terms and Conditions for Use of Self-Archived Versions.
URL	http://hdl.handle.net/2241/00155059

doi: 10.1002/hc.21470

i. Title

Uniquely-folded shapes, photophysical properties, and recognition abilities of macrocyclic BODIPY oligomers

ii. Author names and affiliations

Tomohiro Hojo, Takashi Nakamura, Ryota Matsuoka, Tatsuya Nabeshima*

Graduate School of Pure and Applied Sciences and Tsukuba Research Center for Energy Materials Science (TREMS), University of Tsukuba, 1-1-1 Tennodai, Tsukuba, Ibaraki 305-8571, Japan.

Email: nabesima@chem.tsukuba.ac.jp

iii. Abstract

Macrocyclic BODIPY/dipyrrin tetramers and pentamers connected by *m*-phenylene linkers were synthesized. Their uniquely-folded shapes were revealed by a single-crystal X-ray diffraction analysis, and their dynamic structural behaviors in solution were investigated by variable-temperature NMR measurements. The BODIPY oligomers exhibited strong emission properties without quenching. Furthermore, the BODIPY pentamer interacted with an ammonium cation utilizing the negatively-charged binding pockets in which the polarized B^{δ+}-F^{δ-} bonds are present.

Dedicated to 82nd birthday of Professor Furukawa

iv. Main text

1. Introduction

BODIPY, the boron complexes of dipyrin, is an important class of organic fluorophores.^[1,2] Among the main group element/transition metal complexes of the dipyrins,^[3-8] BODIPY is the most widely investigated because of its strong visible emission, high stability, and chemical tunability. By introducing appropriate interaction units, the BODIPY derivatives have been utilized as fluorescent sensors of chemical species.^[9,10] The BODIPYs' molecular recognition abilities can be achieved or performed not only by attaching functional units, but also by making a macrocyclic framework composed of multiple BODIPY units. There are some reports about macrocyclic dipyrin oligomers and their group 13 element complexes (B and Al) that capture guest molecules in their cavities.^[11-17] In particular, the BF₂ complexes of the macrocycles recognize cations via multipoint hydrogen bonds and electrostatic interactions with the BF₂ unit.^[12,14] The polarization of the B^{δ+}-F^{δ-} bond resulting from the large difference in the electronegativity of the two elements (B, 2.0; F, 4.0)^[18] is utilized in the formation of the guest-binding pocket.

The arrangement of multiple BODIPY units is an important factor that determines their photophysical properties^[16,17,19-23] and molecular recognition abilities^[12,14,17]. For example, a macrocyclic trimer whose BODIPY units are arranged in a triangular manner exhibited mutual exciton coupling among the chromophores.^[17] In terms of molecular recognition, a macrocyclic bowl-shaped BODIPY trimer binds unsymmetrical axle molecules in a unidirectional manner, utilizing multipoint hydrogen bonds with BF₂ units accumulated on one side of the macrocycle.^[14] Thus, the development of oligomers with the unique arrangement of the BODIPY units leads to interesting novel functions.

We now report uniquely-shaped macrocyclic BODIPY oligomers that are composed of four or five dipyrin/BODIPY units linked by a *m*-phenylene unit (**Figure 1**). The boron complexation reaction of a dipyrin tetramer **D4**^[24] resulted in not only a tetranuclear BF₂ complex **B4**, but also the dinuclear BF₂ complex **B2D2**. **B2D2**, in which the two diagonal dipyrins are selectively converted, has a chair-like shape whose flipping is investigated by variable-temperature NMR (**Figure 3**). The BODIPY pentamer **B5** is folded so as to possess two negatively charged binding pockets surrounded by BF₂ units (**Figure 4**). The photophysical properties and molecular recognition abilities are investigated and discussed in connection with their unique structures.

2. Results and Discussion

2-1. BODIPY-dipyrin tetramer **B2D2** and BODIPY tetramer **B4**

We have previously reported a series of macrocyclic dipyrin oligomers from the dimer **D2'** to pentamer **D5'** linked by a 2,6-*m*-phenylene linker possessing a methoxy group at the 1st position and a methyl group at the 4th position (**Figure 2**).^[15] The *m*-phenylene linker behaves as a rigid connection unit with an angle of ~120°, but possesses some degrees of rotational freedom at the same time. This structural feature leads to the formation of variously-shaped macrocyclic structures. The BODIPY trimer **B3'** and tetramer **B4'** were also synthesized from the corresponding dipyrin oligomers **D3'** and **D4'**, respectively (**Figure 2**).^[15] Considering their use as molecular hosts, however, it was speculated that the methyl group at the 4th position would be unfavorable because it projects into the inner cavity and fills the space. Thus, the *m*-phenylene linker without the methyl group has been utilized in recent studies (see **D3**,^[14] **D4**,^[24] and **B3**^[14] in **Figure 2**).

A macrocyclic dipyrin tetramer **D4** was synthesized by the condensation of 2,6-bis(2-pyrrolyl)anisole and mesitaldehyde according to the literature.^[24] Upon the reaction of **D4**

with $\text{BF}_3 \cdot \text{Et}_2\text{O}$ in the presence of the $\text{NEt}(i\text{-Pr})_2$ base, a tetranuclear boron complex **B4** was synthesized in 69% yield. The complexation reaction was slow compared to the synthesis of the normal BODIPYs, presumably due to the conformation restriction of the dipyrin macrocycle. Adjustment of the reaction condition allowed the formation of a partially complexed dinuclear boron-dipyrin **B2D2** in 70% yield (see the Experimental section). The BODIPY tetramer **B4** was found to possess a four-pointed star shape, which is similar to the previously reported BODIPY tetramer **B4'** containing the *m*-phenylene linker with methyl groups,^[15] thus is not discussed in detail (see the Supporting Information for the X-ray crystallographic data and other spectra). For the dinuclear boron complex **B2D2**, a single-crystal X-ray structure was reported for an analogous compound with a methyl-substituted linker,^[15] but the other characterization data in solution were not provided. An X-ray structure of **B2D2** synthesized in this study is shown in **Figures 3a,b**. It was confirmed that two boron difluoride units are introduced into the diagonal dipyrin units of the macrocyclic tetramer. Two consecutive *m*-phenylene linkers took a conformation whose methoxy group is positioned inward (shown by the blue circle in **Figure 3b**). This conformation is explained by the intramolecular hydrogen bonds between the oxygen of the methoxy group and N-H of the dipyrin units. On the other hand, the conformation of the two other linkers are reversed, i.e., with its methoxy group directed outside (shown by the red circle in **Figure 3b**). As a result, **B2D2** is folded like a chair in which one BODIPY unit constitutes its “seating face” and the other constitutes the “backrest”.

Interestingly, the folded shape of **B2D2** observed in the crystal is retained in the solution state. Four different signals were observed in the ^{19}F NMR spectrum of a CDCl_3 solution of **B2D2** at 273 K (−116.8, −123.9, −149.0, and −150.8 ppm) (**Figure 3c**). This agrees with the symmetry of the chair-like conformation of **B2D2**, whose two BF_2 units are in different environments with each having two non-equivalent F atoms. To investigate the

dynamic behavior of **B2D2** in solution, the ^1H NMR spectra were measured at different temperatures (**Figures 3d–3g**, Figure S16). The symmetry suggested from the spectrum at low temperature (248 K) matched with the one observed in the crystal. Meanwhile, the signals became broad and coalesced at elevated temperatures. The activation energy parameters for the conformational change in which two different *m*-phenylene linkers were exchanged were determined from the line shape analyses of the ^1H NMR signals of the methoxy groups and the Eyring plot (Figure S17). The activation enthalpy ΔH^\ddagger was determined to be $39.7 \text{ kJ}\cdot\text{mol}^{-1}$ and the activation entropy ΔS^\ddagger was determined to be $-80.4 \text{ J}\cdot\text{mol}^{-1}\cdot\text{K}^{-1}$. Thus, a large activation barrier both in terms of enthalpy and entropy exists for the structural reorganization of the folded **B2D2**. The stable folding of **B2D2** might be the reason for the successful selective introduction of two BF_2 units at the diagonal position of the dipyrin tetramer **D4**.

2-2. BODIPY pentamer **B5**

A macrocyclic dipyrin pentamer **D5** is produced under the same reaction conditions in order to synthesize the tetramer **D4**, and isolated in 9% yield by means of gel permeation chromatography. The following reaction of **D5** with $\text{BF}_3\cdot\text{Et}_2\text{O}$ produced the BODIPY pentamer **B5** in 54% yield (**Figure 4a**). In the ^1H NMR spectra (CDCl_3 , 298 K), signals corresponding to one repeating unit was observed, thus **B5** has a time-averaged 5-fold symmetry on the NMR timescale (Figure S9). In the ^{19}F NMR measurement, a broad signal was observed at -134.3 ppm , which suggests that the conformational exchange of **B5** took place almost on the NMR timescale (Figure S12). Interestingly, the structure of **B5** determined by a crystallographic analysis was found to be twisted in a peculiar and unsymmetrical manner (**Figures 4b,c**). The folded macrocycle can be divided into two parts. One part is comprised of three BODIPY units, and forms a bowl-shaped circular

framework which resembles that of the previously reported BODIPY trimer **B3**^[14]. The other part with two BODIPY units makes a loop-like structure and is projected toward the convex face of the bowl-shaped trimeric part. Although the overall macrocyclic framework is twisted, all five BF₂ units are directed inward. As the result of the accumulation of polarized B^{δ+}-F^{δ-} bonds, **B5** possesses two negatively-charged pockets surrounded by three and two BF₂ units, respectively (**Figures 4d,e**).

2-3. Spectroscopic properties

BODIPY oligomers maintain their strong emission properties despite multiple fluorophores being linked together. Spectroscopic data of the synthesized dipyrins and BODIPYs (**B4**, **B2D2**, **D5**, and **B5**) in CHCl₃ are summarized in **Table 1**. The reported values of the BODIPY trimer **B3**^[14] and monomeric counterpart **1**^[25] are also shown for comparison. The emission quantum yields Φ_F of **B4** and **B5** are as high as 0.83 and 0.91, respectively. On the other hand, emissions from the oligomers containing dipyrin units (**B2D2** and **D5**) are mostly quenched.

Comparing the properties depending on the number of repeating units, the absorption maximum λ_{abs} shifts to a longer wavelength as the BODIPY macrocycle becomes larger, and approaches the value of the monomer analogue **1**. One possible explanation for this phenomenon is that the expansion of the macrocycles leads to a higher degree of freedom in the *m*-phenylene linkers. That is, the contribution from a local conformation in which a BODIPY unit and a linker is coplanar might become greater in the larger oligomers.

2-4. Binding of ammonium cation

Focusing on the two negatively-charged pockets of the uniquely-folded pentamer **B5**, it has the potential for a multimolecular recognition. In this study, binding of the

dibutylammonium cation $\mathbf{2}^+$ was investigated by ^1H NMR (**Figure 5**).^[12,14] Upon the incremental addition of $\mathbf{2}^+$ into a CDCl_3 solution of **B5** at 298 K, the ^1H NMR signals of **B5** shifted in a two-step manner (Figure S22). For example, the methoxy signal (*h*) shifted upfield during 0–1 equivalents of $\mathbf{2}^+$, while it shifted downfield after 1 equivalent. This suggests that two molecules of $\mathbf{2}^+$ interact with **B5**, and the first binding event is dominant during the 0–1 equivalent addition of $\mathbf{2}^+$, followed by a second binding after 1 equivalent.

The two-step binding constants were determined to be $\log K_1 = 6.7 \pm 1.0$ and $\log K_2 = 3.0 \pm 0.1$ [$\log(\text{M}^{-1})$] from a least square fitting analysis of the ^1H NMR signals during titration (**Figure 5b**). Thus, the first binding is far stronger than the second binding, and a negative cooperative effect is observed. This result is consistent with a Job's plot analysis (Figure S25), which suggests that the 1:1 binding between **B5** and $\mathbf{2}^+$ is dominant under the investigated conditions.

The investigation of the detailed structures of the host-guest complex $[\mathbf{B5}\cdot\mathbf{2}]^+$ and $[\mathbf{B5}\cdot\mathbf{2}_2]^{2+}$ was difficult due to some broadening of the ^1H NMR signals at a lower temperature (223 K, Figure S23). That being said, however, it can be speculated that the first $\mathbf{2}^+$ binds to the cavity of the trimeric BODIPY unit of **B5**. The ^1H NMR signal of the terminal proton of the butyl group of the presumably encapsulated $\mathbf{2}^+$, similar to the previously-reported pseudorotaxane of the BODIPY trimer $[\mathbf{2}@\mathbf{B3}]^{+}$ ^[14], was observed at 0.38 ppm at 1.0 eq during the titration experiment at 223 K. This CH_3 signal is upfield shifted due to the shielding effect from the aromatic macrocycle, and implies that the corresponding butyl group is positioned at the concave face of the trimeric BODIPY unit (Figure S23).^[14] It might be that the second binding of $\mathbf{2}^+$ to **B5** occurs at the BODIPY dimeric units, and is weaker due to the electrostatic repulsion between the cationic $\mathbf{2}^+$ and the shallowness of the second binding pocket. Further investigations of the molecular recognition properties of **B5** utilizing its unique shape are currently underway.

3. Conclusions

We have synthesized macrocyclic tetramers and pentamers of the dipyrrens/BODIPYs linked by *m*-phenylene linkers. Reaction of the dipyrren tetramer **D4** with $\text{BF}_3 \cdot \text{Et}_2\text{O}$ produced a BODIPY-dipyrren mixed macrocycle **B2D2** in which two diagonal dipyrren units were selectively complexed. Its uniquely-folded chair-like structure and conformational dynamic were investigated by a single-crystal X-ray diffraction analysis and variable-temperature NMR analysis, respectively. The BODIPY pentamer **B5** is twisted so as to form two negatively-charged binding pockets to which the dibutyl ammonium cation 2^+ was bound. The strong emission property and recognition ability make these macrocycles promising candidates as functional fluorescent sensors. Furthermore, the macrocyclic complexes synthesized in this study, which possess multiple recognition sites, would be useful platforms toward photofunctional molecules and cooperative molecular hosts that capture complex biological molecules.

4. Experimental

4-1. Materials and methods

Unless otherwise noted, the solvents and reagents were purchased from TCI Co., Ltd., FUJIFILM Wako Pure Chemical Co., Kanto Chemical Co., Inc., Nacalai Tesque, Inc. or Sigma-Aldrich Co., and used without further purification. Silica gel column chromatography was performed using Kanto Chemical silica gel 60 N (spherical, neutral). Alumina for the column chromatography was purchased from FUJIFILM Wako Pure Chemical Co. (alumina, activated (about 75 μm)). GPC purification was performed by a JAI LC-9210 II NEXT system with JAIGEL-1HH/2HH columns using CHCl_3 as the eluent.

Measurements were performed at 298 K unless otherwise noted. The ^1H , ^{13}C , ^{11}B , ^{19}F NMR, and other 2D NMR spectra were recorded by a Bruker AVANCE III-600 (600 MHz) spectrometer or a Bruker AVANCE III-400 (400 MHz) spectrometer. Tetramethylsilane was used as the internal standard (δ 0.00 ppm) for the ^1H and ^{13}C NMR measurements. Hexafluorobenzene in CDCl_3 (1 wt%) was used as the external standard (δ -163.0 ppm) for the ^{19}F NMR measurements. $\text{BF}_3 \cdot \text{Et}_2\text{O}$ in CDCl_3 (1 wt%) was used as the external standard (δ 0.0 ppm) for the ^{11}B NMR measurements.

Single-crystal X-ray crystallographic measurements were performed using a Bruker APEX II ULTRA with $\text{MoK}\alpha$ radiation (graphite-monochromated, $\lambda = 0.71073 \text{ \AA}$) at 120 K. The collected diffraction images were processed by a Bruker APEX2. The initial structure was solved using SHELXS-2013^[26] and refined using SHELXL-2016^[27], which were running on Yadokari-XG crystallographic software^[28]. CCDC 1868519–1868521 contain the data for this study. The data can be obtained free of charge from The Cambridge Crystallographic Data Centre via www.ccdc.cam.ac.uk/getstructures.

The MALDI-TOF mass data were recorded by an AB SCIEX TOF/TOF 5800 system.

The UV-Vis spectra were recorded by a JASCO V-660 or V-670 spectrophotometer. The emission spectra were recorded by a JASCO FP-8600 fluorescence spectrophotometer. The absolute fluorescence quantum yields were determined by a Hamamatsu Photonics absolute PL quantum yield measurement system C9920-02. Solvents used for measurements were air-saturated.

Melting points were determined by a Yanaco MP-J3 melting point apparatus. The elemental analysis was performed by a Yanaco MT-6 analyzer with tin boats purchased from Elementar. We appreciate Mr. Ikuo Iida and Mr. Masao Sasaki of the University of Tsukuba for the elemental analyses.

4-2. Synthesis of BODIPY/dipyrrin oligomers

4-2-1. Synthesis of B4

To a stirred solution containing **D4**^[24] (9.8 mg, 6.7 μ mol) and diisopropylethylamine (57 μ L, 0.335 mmol) in toluene (10 mL) was added boron trifluoride diethyl etherate (41.4 μ L, 0.335 mmol). After stirring at 100 °C for 1 h, diisopropylethylamine (57 μ L, 0.335 mmol) and boron trifluoride diethyl etherate (41.4 μ L, 0.335 mmol) were added. During the reaction (6 h), the same portions of diisopropylamine and boron trifluoride diethyl etherate were added twice more. After the reaction, water (30 mL) was added to the reaction mixture, then extracted with CHCl₃ (30 mL \times 3). The combined organic layer was dried over Mg₂SO₄, filtered, and concentrated in vacuo. The obtained residue was purified by column chromatography on silica gel using ethyl acetate / hexane (1:8–1:1) and reprecipitation with THF/hexane to give **B4** as a purple solid (7.7 mg, 4.7 μ mol, 69%): purple solid; m.p. > 290 °C; ¹H NMR (400 MHz, CDCl₃) δ 7.95 (d, J = 7.7 Hz, 8H), 7.32 (t, J = 7.7 Hz, 4H), 7.00 (s, 8H), 6.74 (d, J = 4.2 Hz, 8H), 6.67 (d, J = 4.2 Hz, 8H), 3.57 (s, 12H), 2.39 (s, 12H), 2.24 (s, 24H); ¹¹B NMR (128 MHz, CDCl₃) δ 1.28 (t, J_{B-F} = 31.1 Hz);

^{19}F NMR (376 MHz, CDCl_3) δ -131.5 (br); MALDI-TOF MS m/z $[\text{M}+\text{K}]^+$ calcd for $\text{C}_{100}\text{H}_{84}\text{B}_4\text{F}_8\text{N}_8\text{O}_4\text{K}$ 1695.7, found 1695.5; Elemental analysis, (calc., found) for $\text{C}_{100}\text{H}_{87}\text{B}_4\text{F}_8\text{N}_8\text{O}_{5.5}$ ($(\text{B4})\cdot(\text{H}_2\text{O})_{1.5}$), C (71.32, 71.33), H (5.21, 5.26), N (6.65, 6.57). It was difficult to obtain a good ^{13}C NMR spectrum due to the low solubility of **B4**.

4-2-2. Synthesis of **B2D2**

To a stirred solution of **D4**^[24] (11.3 mg, 7.7 μmol) in toluene (5 mL) were added diisopropylethylamine (26 μL , 0.153 mmol) and boron trifluoride diethyl etherate (19.5 μL , 0.154 mmol). After stirring at 100 $^\circ\text{C}$ for 30 min, the volatile was removed in vacuo. Chloroform was added to the residue, and the organic layer was washed with water (20 mL \times 2). The organic layer was dried over Na_2SO_4 , filtered, and concentrated in vacuo. The obtained residue was purified by column chromatography on silica gel using CHCl_3 to give **B2D2** as a red solid (8.5 mg, 5.4 μmol , 70%). An analytically pure sample was obtained by washing the solid with acetonitrile and hexane: red solid; m.p. > 280 $^\circ\text{C}$; ^1H NMR (600 MHz, CDCl_3 , 223 K) δ 13.87 (s, 2H), 8.61 (d, $J = 7.4$ Hz, 2H), 7.80 (d, $J = 7.4$ Hz, 2H), 7.75 (d, $J = 7.7$ Hz, 2H), 7.64 (d, $J = 7.7$ Hz, 2H), 7.27 (t, $J = 7.4$ Hz, 2H), 7.26 (s, 1H), 7.17 (d, $J = 4.2$ Hz, 2H), 7.12 (s, 1H), 7.06 (s, 1H), 7.05 (d, $J = 4.2$ Hz, 2H), 7.03 (s, 1H), 6.96 (t, $J = 7.7$ Hz, 2H), 6.92 (s, 2H), 6.90 (s, 2H), 6.77 (d, $J = 4.2$ Hz, 2H), 6.74 (d, $J = 4.2$ Hz, 2H), 6.65–6.64 (m, 4H), 6.60 (d, $J = 4.2$ Hz, 2H), 6.15 (m, 2H), 3.49 (s, 6H), 3.35 (s, 6H), 2.52 (s, 3H), 2.46 (s, 3H), 2.45 (s, 3H), 2.43 (s, 3H), 2.42 (s, 3H), 2.35 (s, 6H), 2.14 (s, 6H), 2.13 (s, 3H), 2.09 (s, 6H); ^{13}C NMR (151 MHz, CDCl_3 , 223 K) δ 164.3, 157.3, 154.8, 154.6, 154.5, 148.2, 144.8, 143.8, 138.7, 138.4, 138.0, 137.2, 137.0, 136.8, 136.6, 136.4, 136.3, 136.1, 135.3, 135.1, 134.3, 133.4, 132.7, 132.6, 130.5, 129.9, 129.9, 129.8, 129.4, 128.9, 128.5, 128.2, 128.0, 127.9, 127.7, 127.4, 125.7, 124.2, 123.2, 123.2, 121.7, 121.6, 120.9, 109.9, 61.6, 61.5, 21.3, 21.2, 20.4, 20.2, 20.2, 19.8, 18.8. Some signals overlapped

each other under this resolution (there exist 60 different ^{13}C in **B2D2**). See Figure S5 for the ^{13}C NMR spectrum; ^{11}B NMR (128 MHz, CDCl_3) δ 1.06 (t, $J_{\text{B-F}} = 30.5$ Hz); ^{19}F NMR (565 MHz, CDCl_3 , 273 K) δ -116.8 (doublet of 1:1:1:1 quartet, $J_{19\text{F}-19\text{F}} = 96.7$ Hz, $J_{11\text{B}-19\text{F}} = 30.5$ Hz), -123.9 (doublet of 1:1:1:1 quartet, $J_{19\text{F}-19\text{F}} = 96.7$ Hz, $J_{11\text{B}-19\text{F}} = 30.5$ Hz), -149.0 (doublet of 1:1:1:1 quartet, $J_{19\text{F}-19\text{F}} = 93.5$ Hz, $J_{11\text{B}-19\text{F}} = 30.5$ Hz), -150.8 (doublet of 1:1:1:1 quartet, $J_{19\text{F}-19\text{F}} = 93.5$ Hz, $J_{11\text{B}-19\text{F}} = 30.5$ Hz); MALDI-TOF MS m/z $[\text{M}+\text{H}]^+$ calcd for $\text{C}_{100}\text{H}_{87}\text{B}_2\text{F}_4\text{N}_8\text{O}_4$ 1562.7, found 1562.8; Elemental analysis (calcd, found) for $\text{C}_{100}\text{H}_{87}\text{N}_8\text{O}_{4.5}\text{B}_2\text{F}_4$ (**B2D2**• $(\text{H}_2\text{O})_{0.5}$); C (76.48, 76.58), H (5.58, 5.63), N (7.14, 7.04).

4-2-3. Synthesis of D5

To a stirred solution containing 2,6-bis(2-pyrrolyl)anisole^[14] (963.5 mg, 4.04 mmol) and mesitaldehyde (670 μL , 4.62 mmol) in dichloromethane (300 mL) was added trifluoroacetic acid (707 μL , 9.23 mmol) under an argon atmosphere. The mixture was stirred at room temperature in the dark for 50 h. 2,3-Dichloro-5,6-dicyano-*p*-benzoquinone (979.4 mg, 4.31 mmol) was added and the resulting solution was stirred in the dark for another 1.5 h. Triethylamine (4.7 mL, 34 mmol) was then added and the resulting solution was stirred in the dark for another 18 h. The reaction mixture was directly loaded on the top of an alumina column and eluted with dichloromethane. The first eluting red band was collected and concentrated in vacuo. The resultant red solid was further purified by GPC to give 135.5 mg of **D5** (73.9 μmol , 9%): red solid; m.p. > 280 $^\circ\text{C}$; ^1H NMR (600 MHz, CDCl_3) δ 14.0 (br, 5H), 8.05 (d, $J = 7.5$ Hz, 10H), 7.13 (t, $J = 7.5$ Hz, 5H), 6.97 (d, $J = 3.9$ Hz, 10H), 6.95 (s, 10H), 6.52 (d, $J = 3.9$ Hz, 10H), 3.71 (s, 15H), 2.35 (s, 15H), 2.25 (s, 30H); ^{13}C NMR (101 MHz, CDCl_3) δ 156.7, 141.2, 138.6, 137.4, 136.9, 133.5, 129.6, 127.9, 127.8, 124.9, 118.9, 61.7, 21.2, 20.2. Some ^{13}C NMR signals were severely broadened due to the chemical exchange at a rate similar to the NMR timescale; MALDI-TOF MS m/z

$[M+H]^+$ calcd for $C_{125}H_{111}N_{10}O_5$ 1832.9, found 1832.6; Elemental analysis, (calcd, found) for $C_{125}H_{112}N_{10}O_6$ (**D5**·(H₂O)), C (81.14, 81.09), H (6.10, 6.17), N (7.57, 7.44).

4-2-4. Synthesis of **B5**

To a stirred solution containing **D5** (23.2 mg, 12.7 μ mol) and diisopropylethylamine (108 μ L, 0.635 mmol) in toluene (10 mL) was added boron trifluoride diethyl etherate (78.4 μ L, 0.635 mmol). After stirring at 100 °C for 30 min, water was added to the reaction mixture, then extracted with CHCl₃ (20 mL \times 2). The combined organic layer was dried over Na₂SO₄, filtered, and concentrated in vacuo. The obtained residue was purified by column chromatography on silica gel using chloroform to give **B5** as a purple solid (14.2 mg, 6.86 μ mol, 54%): red solid; m.p. > 280 °C; ¹H NMR (400 MHz, CDCl₃, 298 K) δ 7.89 (d, J = 7.8 Hz, 10H), 7.28 (t, J = 7.8 Hz, 5H), 6.97 (s, 10H), 6.64 (d, J = 4.4 Hz, 10H), 6.62 (d, J = 4.4 Hz, 10H), 3.45 (s, 15H), 2.38 (s, 15H), 2.19 (s, 30H); ¹³C NMR (101 MHz, CDCl₃) δ 157.5, 155.0, 143.3, 138.4, 136.7, 135.8, 133.3, 130.5, 128.4, 128.1, 125.9, 123.2, 122.6, 61.9, 21.2, 20.1; ¹¹B NMR (128 MHz, CDCl₃) δ 1.17 (t, J_{B-F} = 31.1 Hz); ¹⁹F NMR (376 MHz, CDCl₃) δ -134.3 (br); MALDI-TOF MS m/z $[M+H]^+$ calcd for $C_{125}H_{106}B_5F_{10}N_{10}O_5$ 2071.9, found 2071.8; Elemental analysis, (calcd, found) for $C_{125}H_{106}B_5F_{10}N_{10}O_{5.5}$ (**B5**·(H₂O)_{0.5}); C (72.17, 72.08), H (5.14, 5.22), N (6.73, 6.60).

4-3. Binding studies of ammonium cation

2(TFPB) was prepared according to the literature.^[14] Initial sample solution; [**B5**] = 1.0 mM in CDCl₃, 500 μ L. Titrating stock solution; [**B5**] = 1.0 mM, [**2**(TFPB)] = 12.5 mM in CDCl₃. The stock solution was titrated into the sample solution and then ¹H NMR measurements were performed (223 K and 298 K) (Figures S22 and S23). The two-step

binding constants K_1 and K_2 were determined from the least square fittings of the chemical shift changes of **B5** at 298 K using the TitrationFit software^[29].

v. References

1. A. Loudet, K. Burgess, *Chem. Rev.* **2007**, *107*, 4891–4932.
2. G. Ulrich, R. Ziessel, A. Harriman, *Angew. Chem. Int. Ed.* **2008**, *47*, 1184–1201.
3. H. Maeda, *Eur. J. Org. Chem.* **2007**, 5313–5325.
4. S. A. Baudron, *Dalton Trans.* **2013**, *42*, 7498–7509.
5. T. Nabeshima, M. Yamamura, G. J. Richards, T. Nakamura, *J. Synth. Org. Chem., Jpn.* **2015**, *73*, 1111–1119.
6. N. Sakamoto, C. Ikeda, M. Yamamura, T. Nabeshima, *J. Am. Chem. Soc.* **2011**, *133*, 4726–4729.
7. M. Yamamura, H. Takizawa, N. Sakamoto, T. Nabeshima, *Tetrahedron Lett.* **2013**, *54*, 7049–7052.
8. M. Yamamura, M. Albrecht, M. Albrecht, Y. Nishimura, T. Arai, T. Nabeshima, *Inorg. Chem.* **2014**, *53*, 1355–1360.
9. N. Boens, V. Leen, W. Dehaen, *Chem. Soc. Rev.* **2012**, *41*, 1130–1172.
10. S. Kolemen, E. U. Akkaya, *Coord. Chem. Rev.* **2018**, *354*, 121–134.
11. C. Ikeda, N. Sakamoto, T. Nabeshima, *Org. Lett.* **2008**, *10*, 4601–4604.
12. N. Sakamoto, C. Ikeda, T. Nabeshima, *Chem. Commun.* **2010**, *46*, 6732–6734.
13. M. Saikawa, M. Daicho, T. Nakamura, J. Uchida, M. Yamamura, T. Nabeshima, *Chem. Commun.* **2016**, *52*, 4014–4017.
14. T. Nakamura, G. Yamaguchi, T. Nabeshima, *Angew. Chem. Int. Ed.* **2016**, *55*, 9606–9609.
15. J. Uchida, T. Nakamura, M. Yamamura, G. Yamaguchi, T. Nabeshima, *Org. Lett.* **2016**, *18*, 5380–5383.
16. X.-S. Ke, T. Kim, J. T. Brewster, II, V. M. Lynch, D. Kim, J. L. Sessler, *J. Am. Chem. Soc.* **2017**, *139*, 4627–4630.

17. X.-S. Ke, T. Kim, V. M. Lynch, D. Kim, J. L. Sessler, *J. Am. Chem. Soc.* **2017**, *139*, 13950–13956.
18. A. L. Allred, *J. Inorg. Nucl. Chem.* **1961**, *17*, 215–221.
19. T. Sakida, S. Yamaguchi, H. Shinokubo, *Angew. Chem. Int. Ed.* **2011**, *50*, 2280–2283.
20. M. Ishida, T. Omagari, R. Hirosawa, K. Jono, Y. M. Sung, Y. Yasutake, H. Uno, M. Toganoh, H. Nakanotani, S. Fukatsu, D. Kim, H. Furuta, *Angew. Chem. Int. Ed.* **2016**, *55*, 12045–12049.
21. F. Zinna, T. Bruhn, C. A. Guido, J. Ahrens, M. Bröring, L. Di Bari, G. Pescitelli, *Chem. Eur. J.* **2016**, *22*, 16089–16098.
22. M. Tsuchiya, R. Sakamoto, M. Shimada, Y. Yamanoi, Y. Hattori, K. Sugimoto, E. Nishibori, H. Nishihara, *Chem. Commun.* **2017**, *53*, 7509–7512.
23. L. J. Patalag, L. P. Ho, P. G. Jones, D. B. Werz, *J. Am. Chem. Soc.* **2017**, *139*, 15104–15113.
24. T. Hojo, R. Matsuoka, T. Nabeshima, *Inorg. Chem.* accepted. Please refer to the manuscript and the supporting information of this paper that were uploaded separately as “Supplementary Material for Review”.
25. N. Sakamoto, C. Ikeda, M. Yamamura, T. Nabeshima, *Chem. Commun.* **2012**, *48*, 4818–4820.
26. G. M. Sheldrick, *Acta Cryst.* **2008**, *A64*, 112–122.
27. G. M. Sheldrick, *Acta Cryst.* 2015, *C71*, 3–8.
28. (a) K. Wakita, *Yadokari-XG, Software for Crystal Structure Analyses*, **2001**; (b) C. Kabuto, S. Akine, T. Nemoto, E. Kwon, *J. Cryst. Soc. Jpn.* **2009**, *51*, 218–224.
29. S. Akine, *TitrationFit, ver 1.1.0, For analysis of titration data in host-guest chemistry*, **2013**. http://chem.s.kanazawa-u.ac.jp/coord/titrationfit_e.html (accessed: November 2018).

vi. Tables

Table 1. Spectroscopic data of dipyrin and BODIPY oligomers synthesized in this study (CHCl₃, 298 K)

	$\varepsilon (\times 10^4)$ [cm ⁻¹ ·M ⁻¹]	λ_{abs} [nm]	λ_{em} [nm]	Stokes shift [cm ⁻¹]	Φ_{F}
B4	25	541	617	2300	0.83
B5	29	548	614	2000	0.91
B2D2	19	520	602	2600	0.001
D5	15	514	597	2700	0.02
B3 ^[14]	20	514	606	2950	0.73
1 ^[25]	4.8	551	600	1500	0.88

vii. Figure

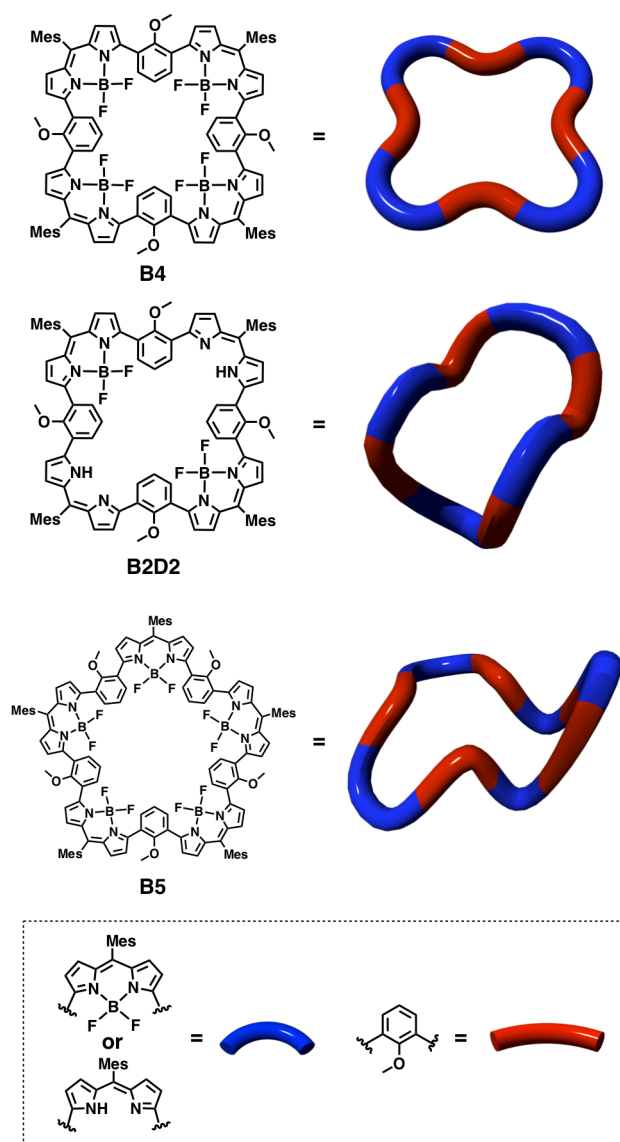


Figure 1. Chemical structures and schematic representation of uniquely-folded BODIPY/dipyrrin oligomers **B4**, **B2D2**, and **B5** (Mes = 2,4,6-trimethylphenyl).

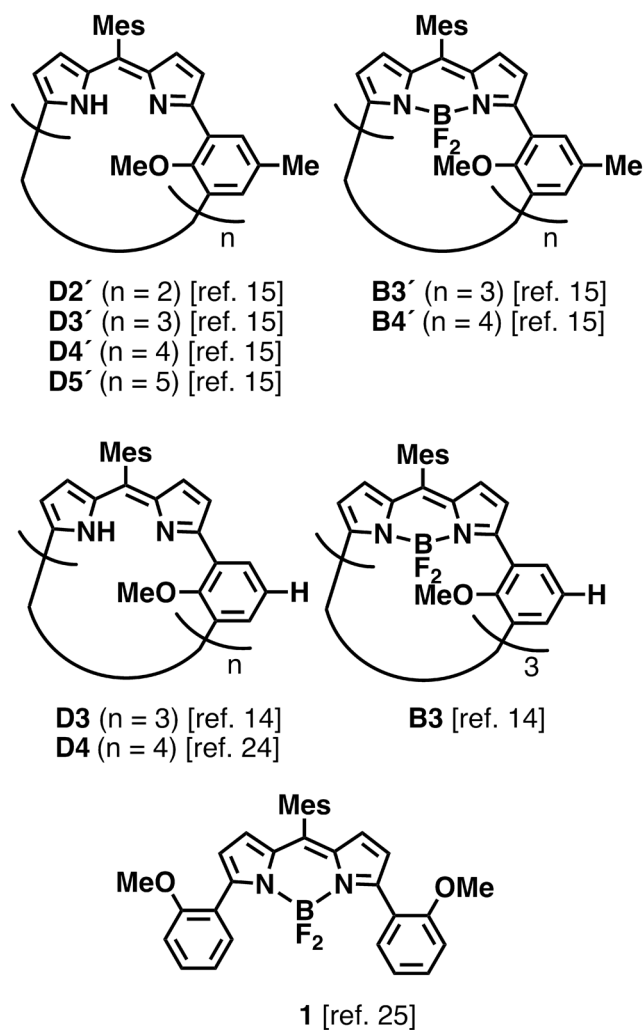


Figure 2. Chemical structures of dipyrin oligomers **D2'**–**D5'**,^[15] BODIPY oligomers **B3'** and **B4'**,^[15] dipyrin oligomers **D3**^[14] and **D4**^[24], BODIPY trimer **B3**^[14], and BODIPY monomer **1**^[25].

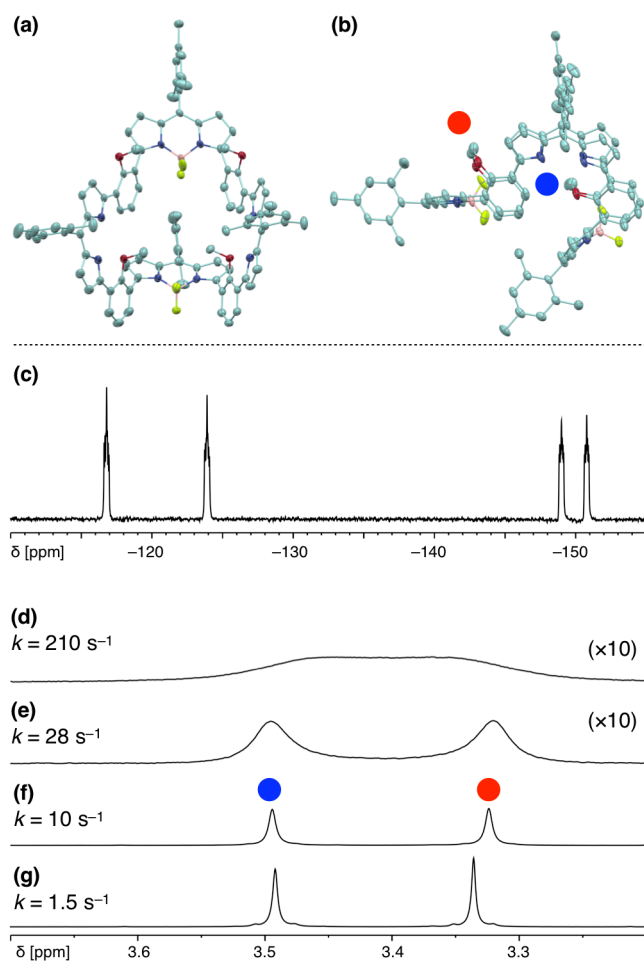


Figure 3. (a,b) The X-ray structure of BODIPY-dipyrrin tetramer **B2D2**. An ellipsoidal model (50% probability). Hydrogen atoms and solvents were omitted for clarity. C, light green; N, blue; O, red; B, pink; F, yellow green. Top view (a) and side view (b). Two kinds of methoxy groups whose NMR signals were employed for the line shape analysis are denoted by the red and blue circles in (b). (c) ^{19}F NMR spectrum of **B2D2** (376 Hz, CDCl_3 , 273 K) (d–g) ^1H NMR signals of methoxy groups of **B2D2** at different temperatures (600 MHz, CDCl_3). (d) 323 K. (e) 298 K. (f) 273 K. (g) 248 K. The rate constants k [s^{-1}] of the exchange between two different methoxy groups determined from the line shape analyses are also given.

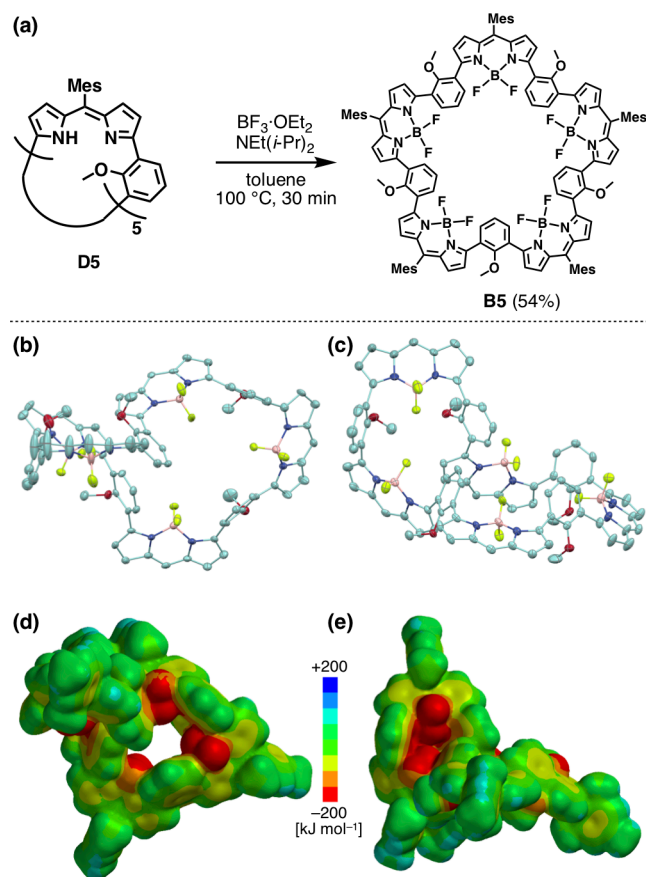


Figure 4. (a) Synthesis of BODIPY pentamer **B5**. (b,c) The X-ray structure of **B5**. An ellipsoidal model (50% probability). Hydrogen atoms, solvents, and Mes groups were omitted for clarity. C, light green; N, blue; O, red; B, pink; F, yellow green. Top view (b) and side view (c). (d,e) Electrostatic potential surfaces of **B5** obtained by DFT calculations at the B3LYP/6-31G* level (the atomic coordinates of the crystal structure of **B5** were used).

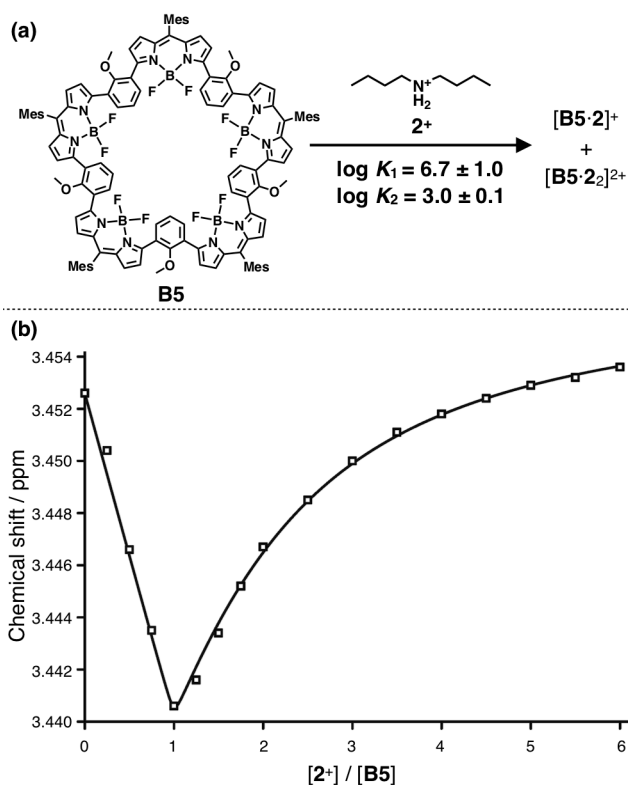


Figure 5. (a) Binding of dibutylammonium cation 2^+ to BODIPY pentamer **B5**. The tetrakis[3,5-bis(trifluoromethyl)phenyl]borate (TFPB) salt of 2^+ was used. The two-step binding constants K_1 and K_2 [M^{-1}] in $CDCl_3$ (298 K) are also shown. (b) A least square fitting to determine K_1 and K_2 between **B5** and 2^+ in a titration experiment ($CDCl_3$, 298 K, $[B5] = 0.995$ mM). The 1H NMR signal of the methoxy group of **B5** was used in the analysis (see Figure S22 for the 1H NMR spectra).